**Fig S1. XFM radiation does not fully quench MitoTracker® Deep Red or ER-Tracker™ Green fluorescence.** Confocal images of control cells labeled with 500 nM MitoTracker® Deep Red (**A**) and 500 nM ER-Tracker™ Green (**B**) were imaged after XFM analysis. White rectangles delineate the area that was imaged during XFM. Scale bar, 50µm.
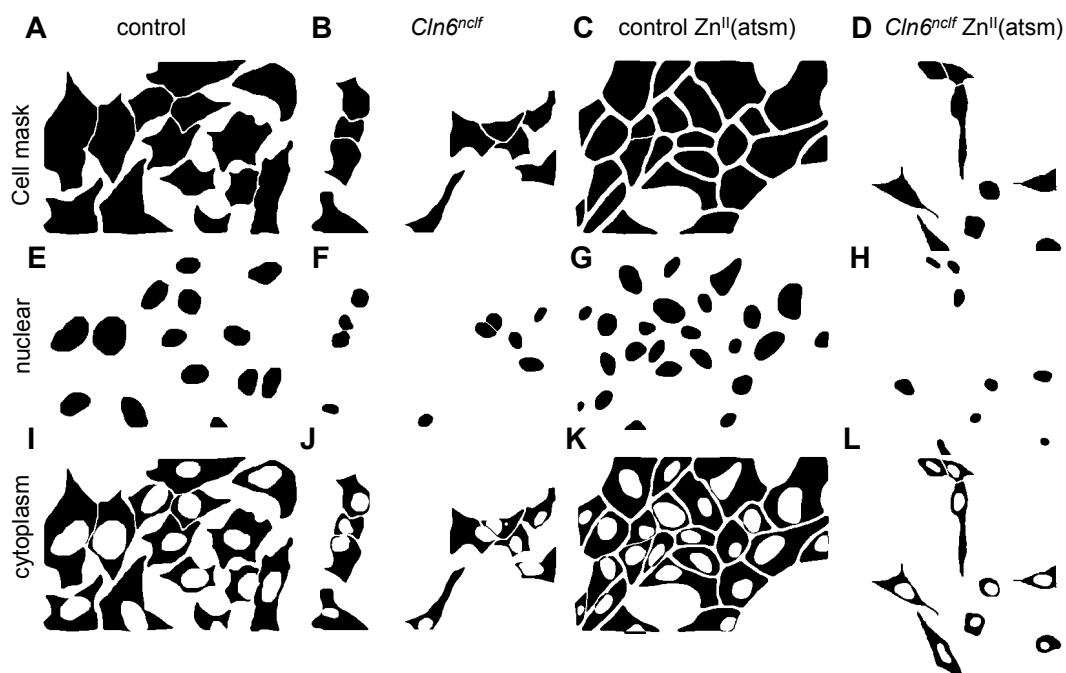


Fig S2. Cellular, nuclear and cytoplasmic masks used for numerical analyses in this study. A-D. Whole cell masks are based on Compton scatter. **E-H**. Nuclear masks were guided by zinc content, zinc/calcium maps and absence of ER and mitochondrial staining. **I-L**. Cytoplasmic masks were designated as cellular non-nuclear area.
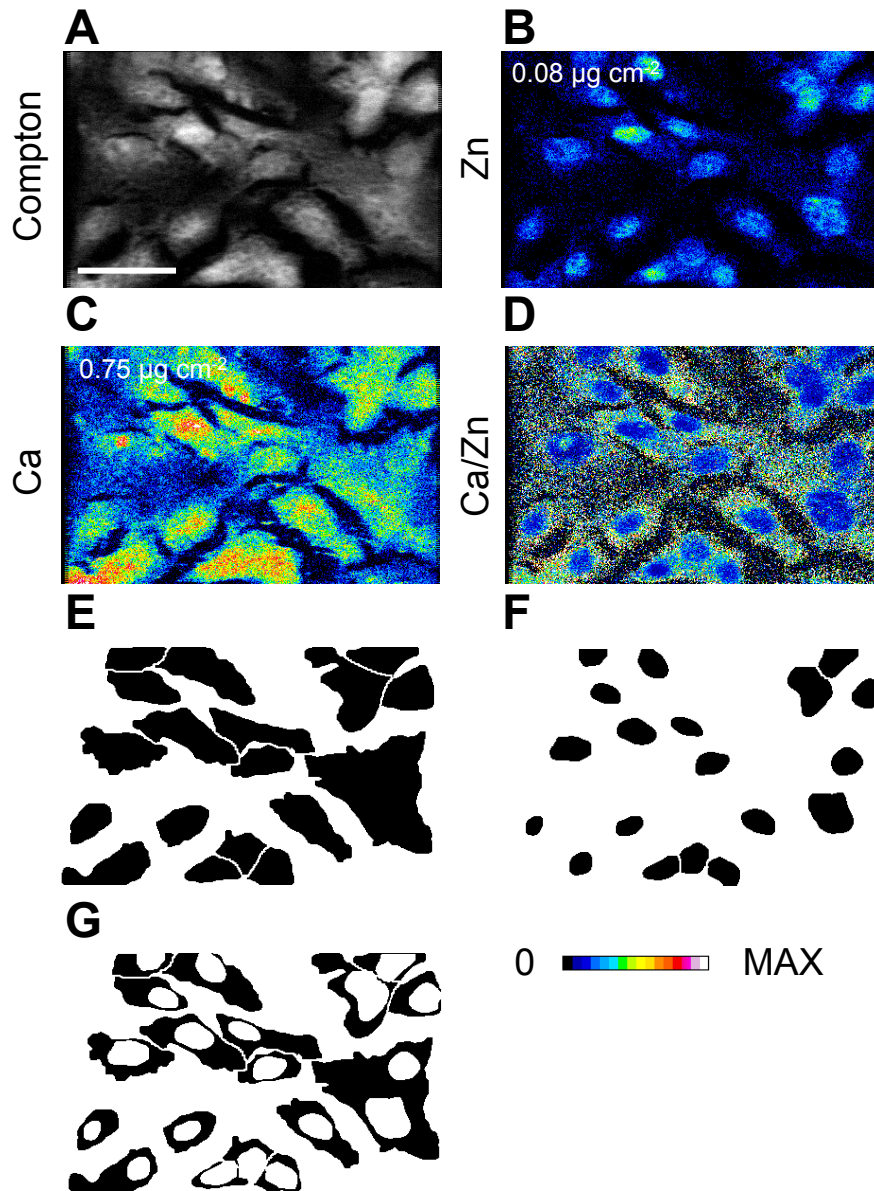
Fig S3. Organelle marker treatment does not perturb cellular zinc or calcium distributions. Cerebellar granule cells from control mice were grown on X-ray transparent SiN windows (500nm thick). Fixed non-stained cells were exposed to an incident beam of 12.7 keV X-rays. **A.** Grayscale-colored images of inelastic scatter (Compton) of incident photons was used to define cell boundaries. **B-C**. Heat maps of elemental concentrations for zinc (**B**) and calcium (**C**). The maximum concentration of each element is shown at the top left of the relevant panel. **D**. Heat map of calcium concentrations divided by zinc concentrations for each pixel. **E**. Whole cell masks of unstained cells are based on Compton scatter. **F**. Nuclear masks were guided by zinc content and zinc/calcium maps. **G**. Cytoplasmic masks were designated as cellular non-nuclear area. Scale bar, 50µm
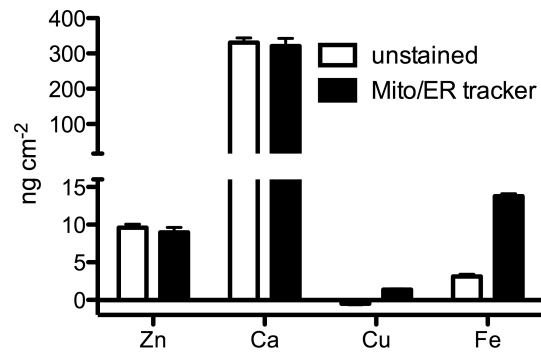
Fig S4. Organelle marker treatment does not perturb cellular zinc or calcium concentrations. The mean concentration of zinc, calcium, copper and iron in each individual unstained (white bars) and organelle marker-stained cell (black bars) was calculated using cell masks constructed in imageJ (Fig S2, S3). Error bars represent SEM.
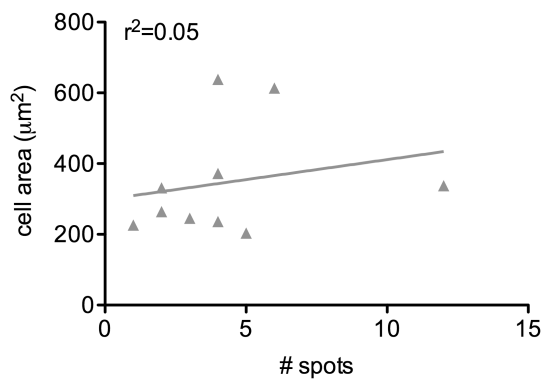
Fig S5. Cellular area does not correlate with the number of calcium deposits per cell. The area of each Cb*Cln6*^{nclf} cell was plotted against the number of deposits with a calcium concentration above 2μg cm^{-2} in that cell.
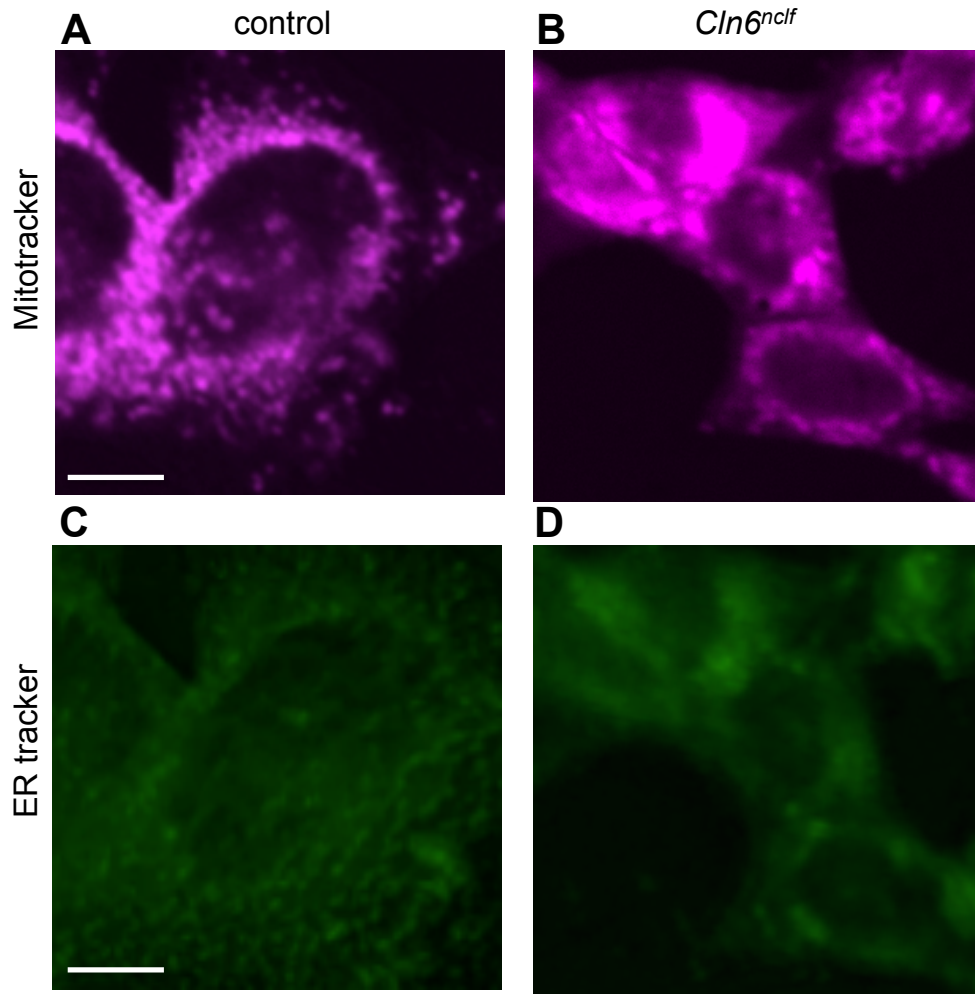
Fig S6. Magnified fluorescence images of MitoTracker® Deep Red and and ER-Tracker™ Green staining in cerebellar cells. Control and *Cln6^{nclf}* cerebellar cells were stained with MitoTracker® Deep Red (500nM; A-B) and ER-Tracker™ Green (500nM; C-D) for 30min prior to fixation. Confocal images depicting subcellular localization of mitochondria and endoplasmic reticulum. Scale bar, 10μm.
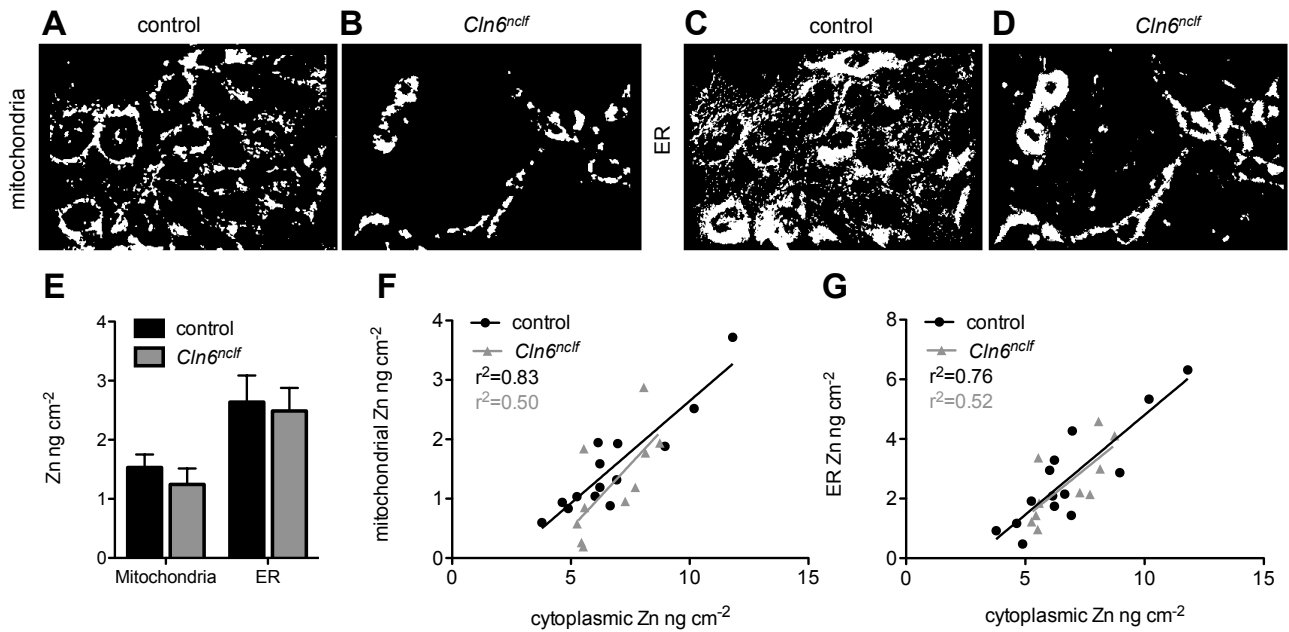
**Fig S7. The mitochondrial and ER zinc distributions are not perturbed in *Cln6^nclf*
cerebellar cells.** Mitochondrial (**A-B**) and ER (**C-D**) masks used for numerical analyses in
this study**.** Masks were constructed from scaled fluorescent images of MitoTracker® Deep
Red and ER-Tracker™ Green-labeled control and *Cln6^nclf* using autolocal Thresholding in
ImageJ by the Bernsen and Phalkansar methods, respectively. **E.** The concentrations of zinc
in the mitochondria and ER of individual cells were calculated by multiplying the elemental
zinc maps by the binary masks and analyzing the metal level in each cytoplasmic cell region.
We excluded nuclear regions from our analysis as the z-plane focus of the X-ray beam is
~500μm, providing a sum of metal content through the depth of the cell, while confocal
images are a z-plane slice of 5 μm. Thus, in the thicker centre of cells, the XFM elemental
maps are likely representative of the metal content present both in the nucleus, and additional
structures in a different z-plane to the nucleus. We therefore excluded the nuclear region
when correlating the mitochondrial (**F**) and ER (**G**) metal content of the cells to cytoplasmic
metal content. Linear regression analysis was performed in GraphPad Prism. r^2 values for the
strength of each correlation are presented in each panel. The linear regressions for
cytoplasmic to ER or mitochondrial zinc were not significantly different between control and
Cln6^nclf cells.